Engineering Structures 195 (2019) 231–242

Contents lists available at ScienceDirect

Engineering Structures

journal homepage: www.elsevier.com/locate/engstruct

Cyclic behavior of squat reinforced concrete walls with openings typical of exterior walls of row houses in Taiwan

Yu-Chen Ou[a,b], Le Hoang[b,c], Hwasung Roh[d,*]

[a] Department of Civil Engineering, National Taiwan University, Taipei, Taiwan
[b] Department of Civil and Construction Engineering, National Taiwan University of Science and Technology, Taipei, Taiwan
[c] Department of Civil Engineering, Can Tho University of Technology, Can Tho, Viet Nam
[d] Department of Civil Engineering, Chonbuk National University, Jeonju, Republic of Korea

ARTICLE INFO

Keywords:
Reinforced concrete
Row houses
Squat walls
Opening
Lateral strength

ABSTRACT

Five full-scale reinforced concrete wall specimens with openings typical of the first story backside exterior walls of row houses in Taiwan were tested using lateral cyclic loading to study their seismic behavior. The effects of location and size of the window opening were studied. Test results showed that the wall with the window opening on the side of the wall web showed a higher average lateral strength than that with the opening placed around the center of the wall web. The increase of the opening length reduced more the lateral strength than the increase of the opening height. A critical wall segment tended to show a lower lateral strength when the edge of the segment is bordered by a door than by a boundary column. To estimate the lateral strength of the wall specimens, a detailed and three simplified models are proposed. Comparison with the test results shows that ignoring variation in the axial force among the wall segments and columns does not change the average prediction but increases the scatter of prediction. Simply summing the lateral strengths of all the wall segments and columns together further increases the scatter and greatly reduces the degree of conservatism. Summing the lateral strengths of all the web segments requires the least computational effort but greatly increases the degree of conservatism.

1. Introduction

Low-rise reinforced concrete (RC) row houses (Fig. 1) are a common building type in Taiwan. During the Chi-Chi Earthquake in 1999, many row houses collapsed due to a weak first story along the street direction (Fig. 2). Today, row houses are built stronger than before with higher material strengths, better reinforcement detailing and larger member dimensions. However, the weak-story problem still exists. This is because walls with openings are usually used for row houses along the street direction (Fig. 1). However, the strengths of such walls are typically ignored in design because the behavior of such walls is not well-understood. Moreover, ignoring the strengths of such walls seems to be on the safe side in design. However, this makes the weak-story check unable to identify the weak story caused by abrupt change of such walls between adjacent stories.

Previous experiment studies on squat walls with openings have shown that when the opening area is small, the behavior of the wall may not be significantly affected [1,2]. When the opening area is large, the initial stiffness and strength of the wall can be significantly reduced [1,2]. However, the ductility may be increased [2]. The reduction in capacity of squat walls depends on the size, shape and location of the opening [3,4]. For example, walls with openings close to the edge or boundary of a wall tend to have lower stiffness and strength than those with openings farther away from the edge or boundary [5]. Slender walls with openings have also been studied [6,7]. The behavior of slender walls with openings tends to be governed by flexure while that of squat walls with openings by shear. An opening centered at the base of slender walls does not significantly affect the lateral strength but can greatly reduce the deformation capacity of the wall [6]. Despite of many test data on squat walls with openings, there are few tests on squat walls with design details similar to those used in exterior walls in the first story and back side of row houses in Taiwan. Many such walls suffered severe damage during the 1999 Chi-Chi earthquake (Fig. 2(b)).

Based on test observation, Ono [3,8] proposed a simple empirical equation to calculate the reduction in shear strength of walls due to openings. The reduction is related to the ratio of the effective area based on an assumed diagonal compression field to the wall area. The Japanese design standard for building structures [9] includes a

* Corresponding author.
E-mail address: hwasung@jbnu.ac.kr (H. Roh).

https://doi.org/10.1016/j.engstruct.2019.05.097
Received 27 November 2018; Received in revised form 28 May 2019; Accepted 28 May 2019

Fig. 1. Low-rise reinforced concrete row houses in Taiwan: (a) front view and (b) back view.

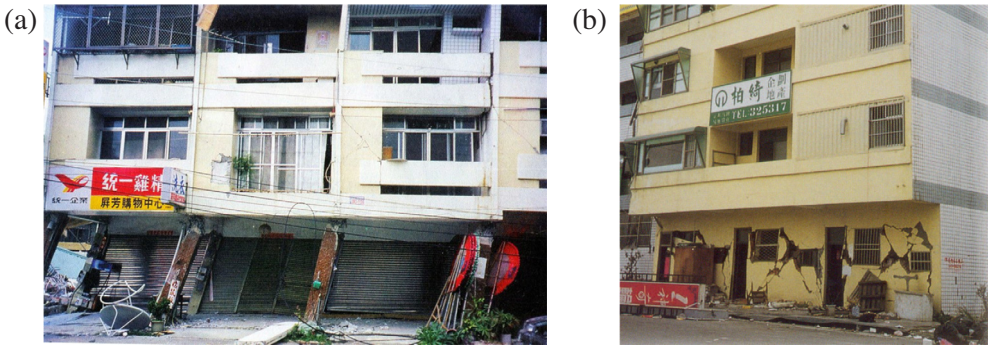

Fig. 2. Weak first story failure along the street direction of row houses in 1999 Chi-Chi Earthquake: (a) front side of a house; (b) back side of a house.

reduction factor for shear strength that considers the effect of the length, area and height of openings. Although these two methods are simple and easy to use, they were developed empirically and cannot realistically consider the failure mechanisms of individual wall segment. Sakurai et al. [10] proposed a simplified shear strength model, in which the shear strength of the wall is the sum of the shear strength contributions from diagonal struts assumed in each wall segment beside openings. Strut-and-tie models have also been developed to predict the strength of walls with openings [2]. While these models can better reflect the change of force transfer mechanism due to openings, they are not easy to be used in design practice.

The objective of this research was to investigate the behavior of squat exterior walls located in the first story and back side of reinforced concrete row houses in Taiwan (Fig. 1(b)). The walls are typically aligned along the street direction and each wall has a door and a window. It may also have an opening for ventilation. However, the opening is usually small and hence not considered in this research. Full-scale wall specimens were constructed and tested using lateral cyclic loading. Methods of calculating the lateral strength of the wall were developed and validated with the test results.

2. Experimental program

2.1. Specimen design

Five full-scale wall specimens were designed based on typical design characteristics of exterior walls in the first story and back side of row houses in Taiwan. The design details of the specimens are shown in Fig. 3. The measured material strengths are listed in Table 1. Each wall specimen had two boundary columns. The length of the wall including the boundary columns was 4600 mm. The height of the wall excluding the loading beam on the top of the wall was 3250 mm. The boundary columns had a cross-sectional dimension of 300 × 500 mm. The short side of the column was placed along the wall length. This is a typical design practice to reduce the interference of the column with the living space of the house. The column was designed based on the design provisions for special moment frames of the ACI 318 code [11] and had a longitudinal reinforcement ratio based on gross concrete area of 1.89% and a transverse reinforcement ratio of 1.82% based on the volume of core concrete. The wall web had a thickness of 15 cm and was designed with two layers of horizontal and vertical reinforcement. The horizontal and vertical reinforcement ratios based on gross concrete area were the same and equal to 0.55%.

Each wall had two openings. The large one was intended to represent a door and the small one for a window. Based on the design practice in Taiwan, the door openings of all the specimens were designed to have a dimension of 2500 × 900 mm and placed beside a boundary column. The dimension and location of the window opening were design variables. The window openings of specimens W1, W2, and W3 had the same size (900 × 900 mm) but were placed in different locations as illustrated in Fig. 3 to investigate the effect of opening location on the wall behavior. The left side of the window opening of specimen W4 was placed in the same location relative to the door as W3. However, the opening was taller (1400 × 900 mm) than that of W3 to investigate the effect of opening height on the wall behavior. The window opening of specimen W5 had a larger length (1400 × 1500 mm) than that of W4 to examine the effect of opening length on the wall behavior. This size of opening approximately represents the maximum size of a window opening typically seen in Taiwan. The total area of openings to the wall area (3250 × 4600 mm) was 0.205, 0.235, and 0.291 for specimens W1-W3, W4, and W5, respectively. Two D16 bars were placed in the wall web around the openings as required by the ACI 318 code [11]. The bars were extended beyond the corners of the openings for 60 cm.

2.2. Test setup

The specimens were tested by lateral cyclic loading to examine their lateral load capacity. Fig. 4(a) and (b) show the test setup. The specimens were fixed to a strong floor by post-tensioning the foundation of the specimen to the strong floor. Lateral cyclic loading was applied to a load transfer beam on the top of the wall by a 2000-kN actuator. The loading was displacement-controlled to drift ratios as shown in Fig. 4(c). The drift ratio is defined as the lateral displacement divided

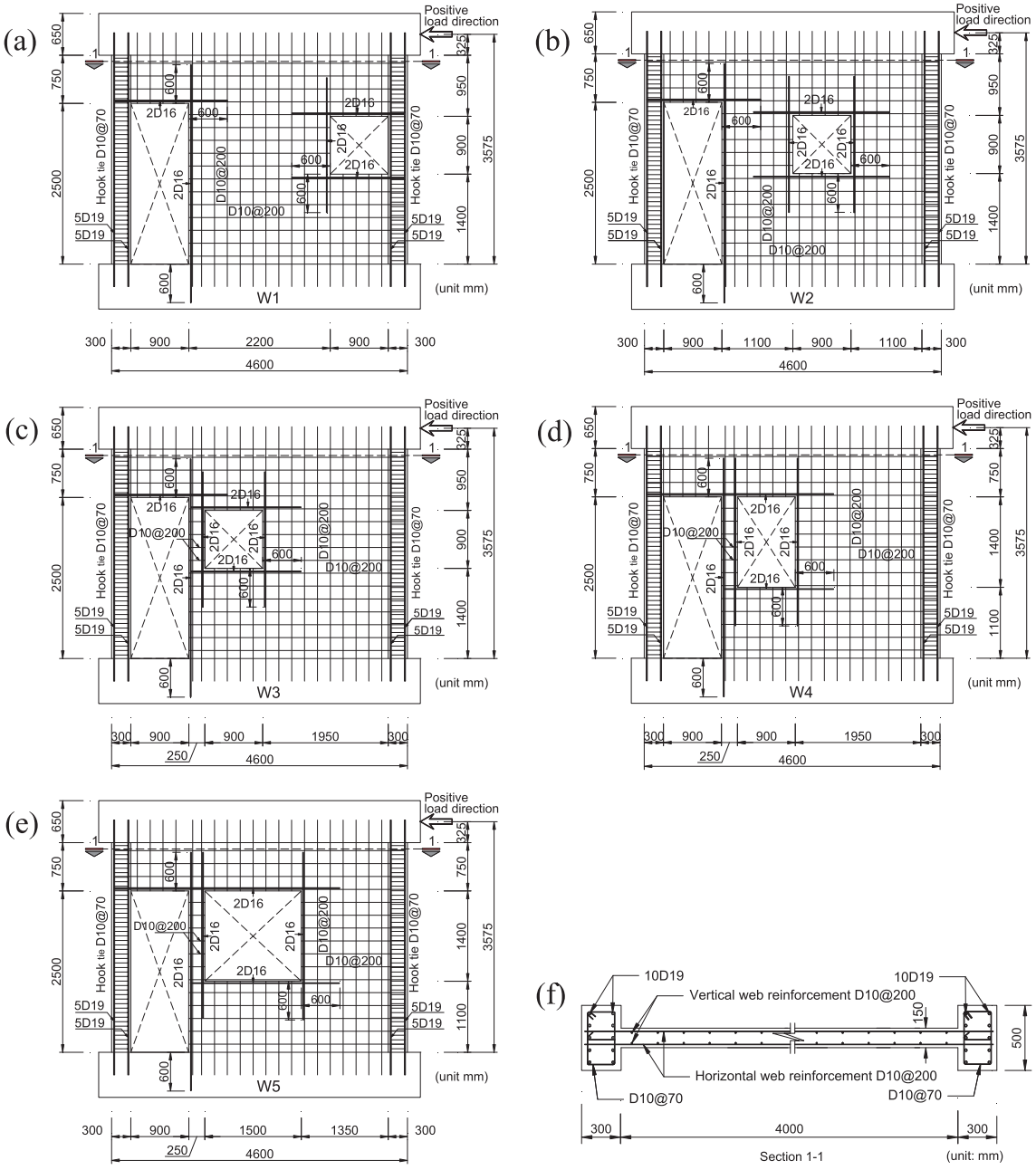

Fig. 3. Specimens design: (a) W1, (b) W2, (c) W3, (d) W4, (e) W5, and (f) section 1-1.

Table 1
Measured properties of materials.

Specimen		W1	W2	W3	W4	W5
Compressive strength of concrete (MPa)		35.6	34.9	37.4	37.3	36.1
Yield strength of steel reinforcement (MPa)	D10			312.8		
	D16			438.4		
	D19			479.2		

by the distance from the loading point to the top of the foundation (3575 mm). Each draft ratio was repeated three times to examine degradation of strength and stiffness under load reversals. No axial load was applied to the specimens. This is because the axial compressive load ratios in columns and walls of real row houses are typically small, less than 10% of $f_c' A_g$, where f_c' = concrete compressive strength; A_g = gross cross-sectional area. Under such a small axial compressive load, it is more conservative in terms of strength to ignore the axial load because a small axial compression is beneficial to flexural, shear and slip resistance of a wall.

2.3. Damage observation

At the first drift level (drifts actually achieved ranging from 0.06 to 0.1%), horizontal cracks occurred in the boundary columns of all the specimens. Some of them extended into the wall web and turned into inclined cracks. At this drift level, cracks also appeared at corners of the window and door. As the drift increased, more inclined cracks occurred in the wall segments beside the boundary columns. Moreover, inclined cracks gradually extended deeper into the center region of the wall web. At drifts ranging from 0.33 to 0.38%, the wall segment in the center region of walls W1 and W2 started to show extensive inclined cracks. Peak lateral forces were reached at drifts of 0.58–1.09%. Fig. 5 shows the crack patterns of all specimens when the peak lateral force had just been reached for both directions.

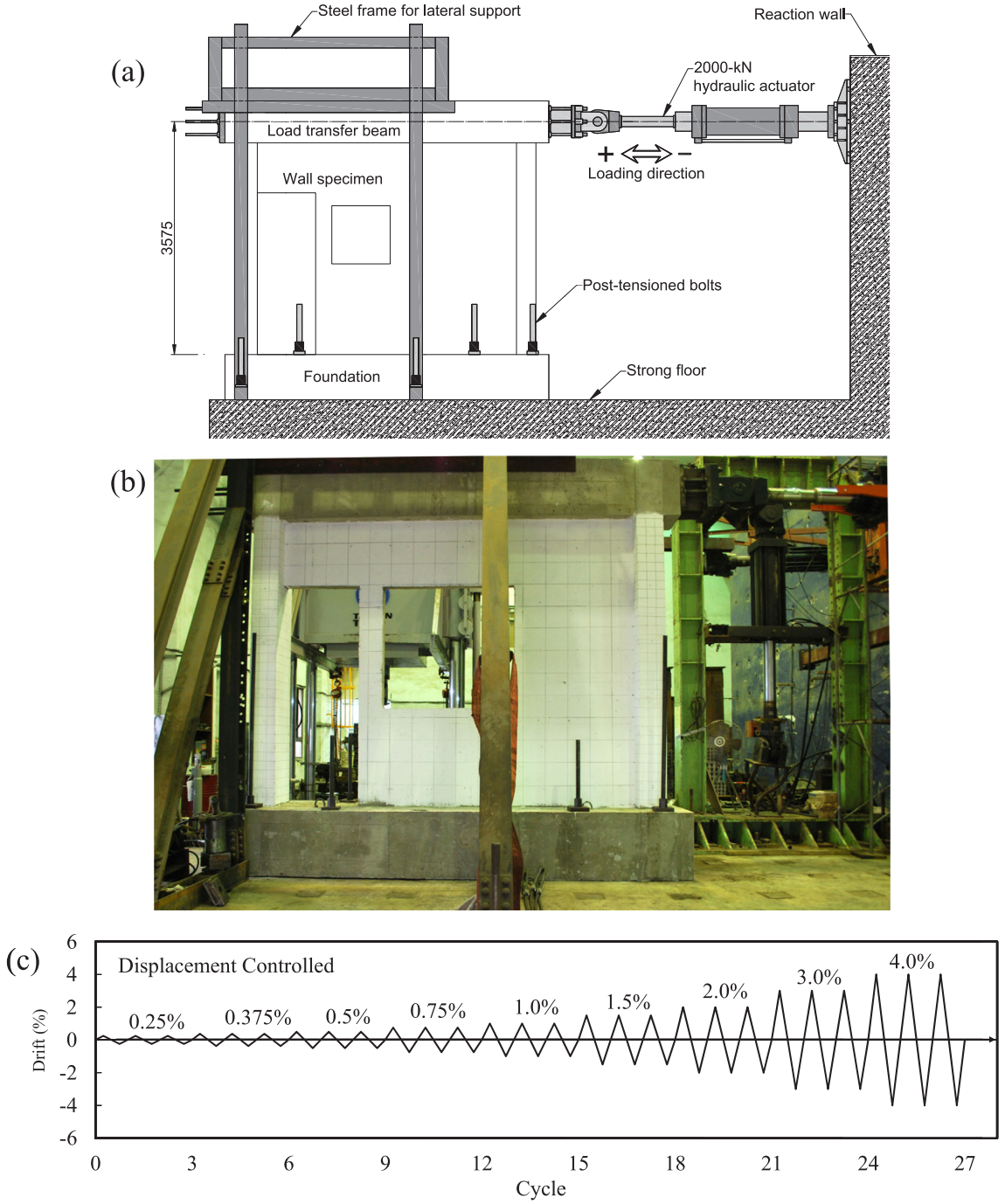

Fig. 4. Cyclic test of specimens: (a) test setup, (b) photo of test setup, and (c) loading protocol.

For each specimen, the peak lateral force was reached when one or multiple inclined cracks suddenly became significantly wider than the other cracks. These cracks are referred to as critical inclined cracks and marked with thicker lines in Fig. 5. The angle to the vertical of the most significant inclined crack is shown in Fig. 5. The angle ranged from 31 to 51 degrees as shown in Fig. 5. Critical inclined cracks tended to occur in or pass through wall segments beside the window, which are referred to as critical wall segments herein. W1 had only one critical wall segment. W2-W5 had two critical wall segments on the two sides of the window. The net horizontal sectional area of the wall was the smallest over the height of the critical segments and hence the damage in these regions was the greatest.

At the drift level next to the peak lateral force (1.12–1.5%), crushing and spalling of concrete was observed along the critical inclined cracks, particularly at the intersection of the critical cracks of different loading directions. As the drift was further increased, the extent of crushing and spalling quickly increased. Tests of W1 and W2 were terminated at drifts of 1.48–1.50% when the critical wall segments had clearly separated into two parts (Fig. 6). The remaining resistance of the specimens were mainly contributed by the two boundary columns. Tests of W3-W5 were terminated later at drifts of 2.54–2.61%. Therefore, more extensive spalling of concrete were observed (Fig. 6) than W1 and W2. At the end of testing, the remaining resistance of W3-W5 was also mainly contributed by the boundary columns. By comparing W1, W2, and W3, it can be seen that the critical inclined cracks (Fig. 5) and damage at the end of testing (Fig. 6) of W2 occurred mostly within the critical wall segments. In contrast, many of the critical cracks and damage of W1 and W3 developed beyond the critical wall segment. By

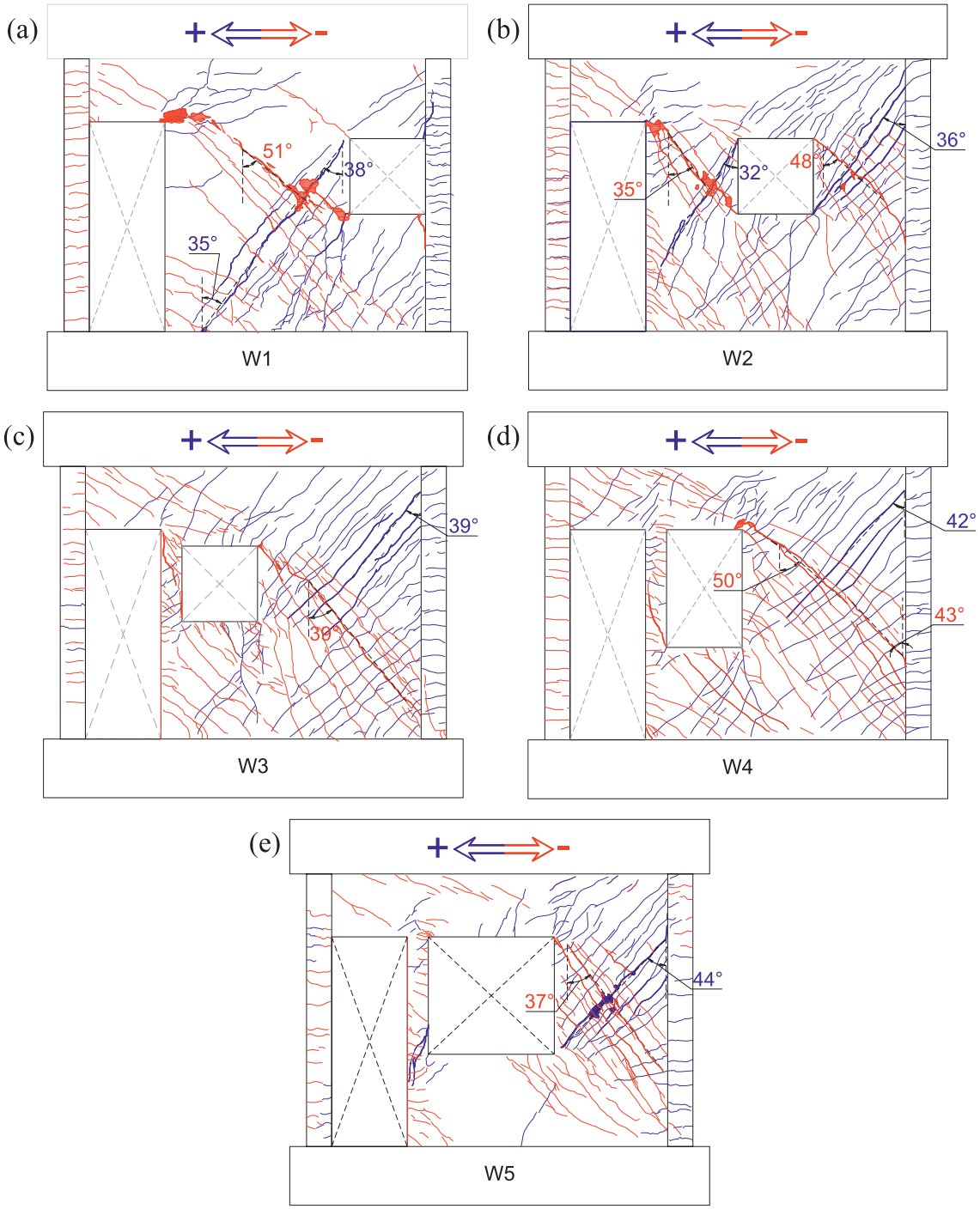

Fig. 5. Crack patterns at peak lateral force: (a) W1 at a drift of −0.92%, (b) W2 at a drift of −0.92%, (c) W3 at a drift of −0.92%, (d) W4 at a drift of −0.93%, and (e) W5 at a drift of + 1.09%.

reducing the size of the critical segment (W4 and W5 compared with W3) and hence reducing the ratio of the strength of the critical segment to those of the adjacent segments, the critical inclined cracks and damage at the end of the testing were confined more within the critical segment.

2.4. Behavior of lateral force and displacement

Fig. 7(a)–(e) show the force-displacement behavior of the specimens. Fig. 7(f) shows the comparison of the envelope responses. The peak lateral forces and corresponding drifts for each loading direction are listed in Table 2. By comparing W1, W2 and W3, it can be seen that the average peak lateral force (average of positive and negative peak lateral forces) of W1 and that of W3 were larger than that of W2. It appeared that moving the window opening from the side of the wall web to the middle of the web reduced the wall resistance. In other words, one large critical wall segment (W1 and W3) had a higher resistance than two smaller segments with a similar total cross-sectional area (W2). This is because the former had a lower height to length ratio than the latter and hence can transfer lateral load more efficiently with a diagonal strut that is less steep. The average peak lateral force of W4 was slightly lower than W3 by 9% even though the height of the

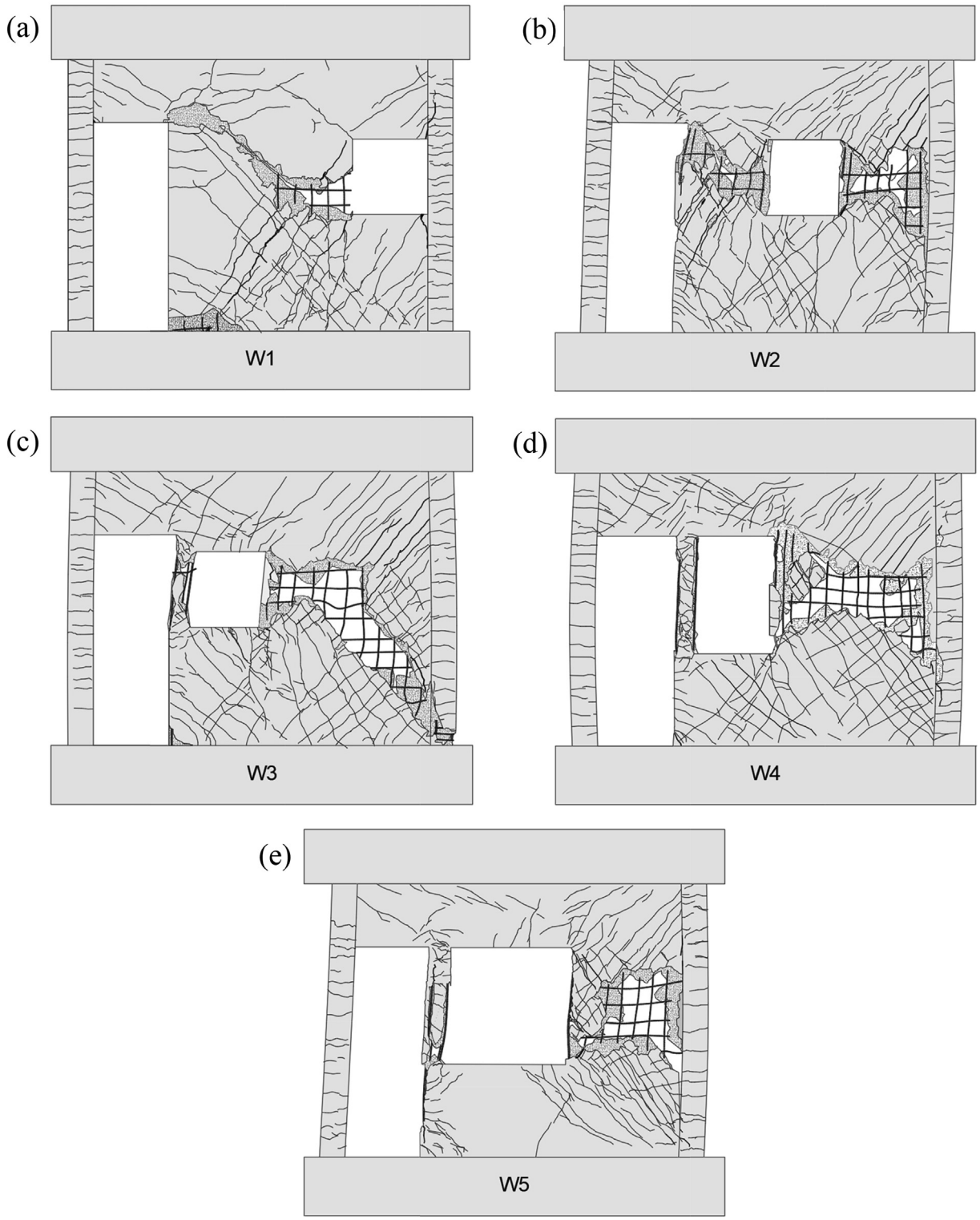

Fig. 6. Damage of specimens at the end of test: (a) W1, (b) W2, (c) W3, (d) W4, and (e) W5.

windows opening was increased by 56%. In contrast, with a 67% increase in the length of the window opening, the average peak lateral force of W5 was greatly reduced by 27% as compared with that of W4. The impact of the length increase of the opening was clearly larger than that of height increase. The height increase increases the height to length ratio of the critical wall segment, which tends to reduce the lateral strength due to load transfer through a steeper diagonal strut. In comparison with the height increase, the length increase not only increases the height to length ratio of the critical wall segment but also reduces the horizontal cross-sectional area of the critical wall segment, which further reduces the lateral strength.

Test results also showed that the peak lateral force in the negative loading direction tended to be higher than that in the positive loading direction (W1, W2, W3, and W5). This is likely because of the confining effect from the boundary column on the right side of the wall web when the wall was loaded in the negative direction. In contrast, when the wall

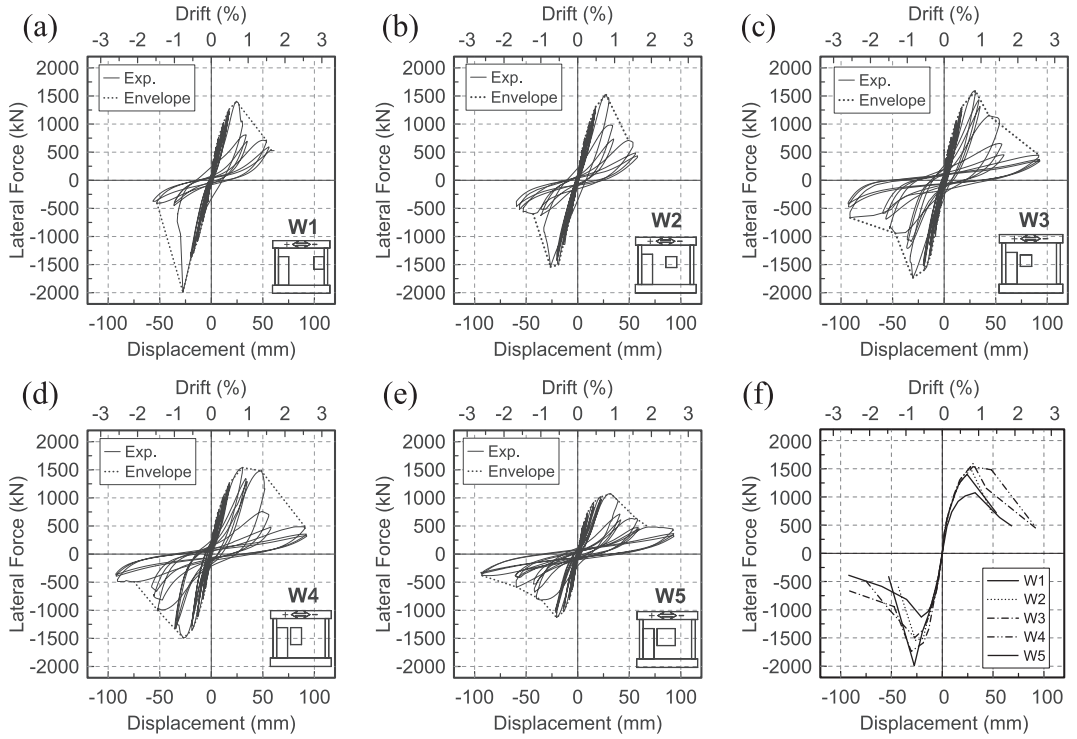

Fig. 7. Hysteretic behavior of specimens: (a) W1, (b) W2, (c) W3, (d) W4, (e) W5, and (f) response envelopes of all specimens.

Table 2
Peak lateral forces and corresponding drifts of specimens.

Specimen	Positive loading		Negative loading	
	Force (kN)	Drift (%)	Force (kN)	Drift (%)
W1	1401.7	0.68	−1989.4	−0.77
W2	1519.5	0.77	−1540.8	−0.74
W3	1593.3	0.85	−1737.7	−0.85
W4	1539.4	0.84	−1493.8	−0.76
W5	1074.4	0.90	−1128.8	−0.58

was loaded in the positive direction, the confining effect from the boundary column on the left side of the wall was greatly reduced by the door opening. It was also noted that W1 in the negative direction showed the highest peak lateral force among all the specimens. It is likely because the openings did not entirely block the diagonal load path from the upper left corner to the lower right corner of the wall web, which is the most effective strut load path. These observations provide a useful guideline in selecting the window location in terms of reducing the effect of the opening on the lateral resistance of the wall.

2.5. Strain measurement

Fig. 8 shows the strain readings of reinforcement in the wall web at the peak lateral force for each loading direction. The strain gauges in the transverse reinforcement tended to show large tensile strains around critical inclined cracks. Several of them in the critical wall segments showed strains exceeding or close to the yield strain. Large tensile strains were also found outside the critical wall segment as the critical inclined cracks were not limited within the critical wall segment. Yielding of longitudinal reinforcement was also observed, particularly in the region when the boundary column nearby was subjected to tension under lateral load.

3. Lateral strength prediction

3.1. Structural model

The calculation of the lateral strength of walls with large openings such as those examined in this research is more complicated than solid walls or walls with small openings. This is because large openings separate a wall into members that tend to behave independently to each other. In such a case, it is more appropriate to model the wall with a structure composing members separated by openings rather than to model the wall as one wall member with the section area reduced by openings. As stated previously, critical wall segments between openings or between an opening and the wall edge tended to show greater damage (Figs. 5 and 6) and higher reinforcement strains (Fig. 8) at the peak lateral force than the other part of the wall. Based on this observation, a structural model as shown in Fig. 9 was proposed to calculate the lateral strength of the walls. In the proposed model, the critical wall segment and the part of the boundary column beside an opening are modeled using vertical frame elements, which are fixed at the top and bottom to rigid elements representing the other regions of the wall. Under lateral load, the vertical elements will have the same lateral displacement at the top and are assumed to have the moment point of inflection at the midheight of the element. The strength and deformation characteristics of each vertical element are calculated based on models presented in the following sections.

3.2. Flexural strength

The flexural strengths of each vertical frame element are calculated for the flexural cracking, yielding and ultimate conditions. The flexural cracking strength is the strength when the maximum tensile stress equal to the modulus of rupture. The flexural yield strength is the strength when the first yielding of longitudinal tension reinforcement occurs. The flexural ultimate strength is the nominal flexural strength M_n as defined by the ACI code [11] when the maximum concrete compressive strain reaches 0.003. Concrete is assumed to be unconfined and reinforcement is assumed to have elastic-perfectly plastic behavior. When

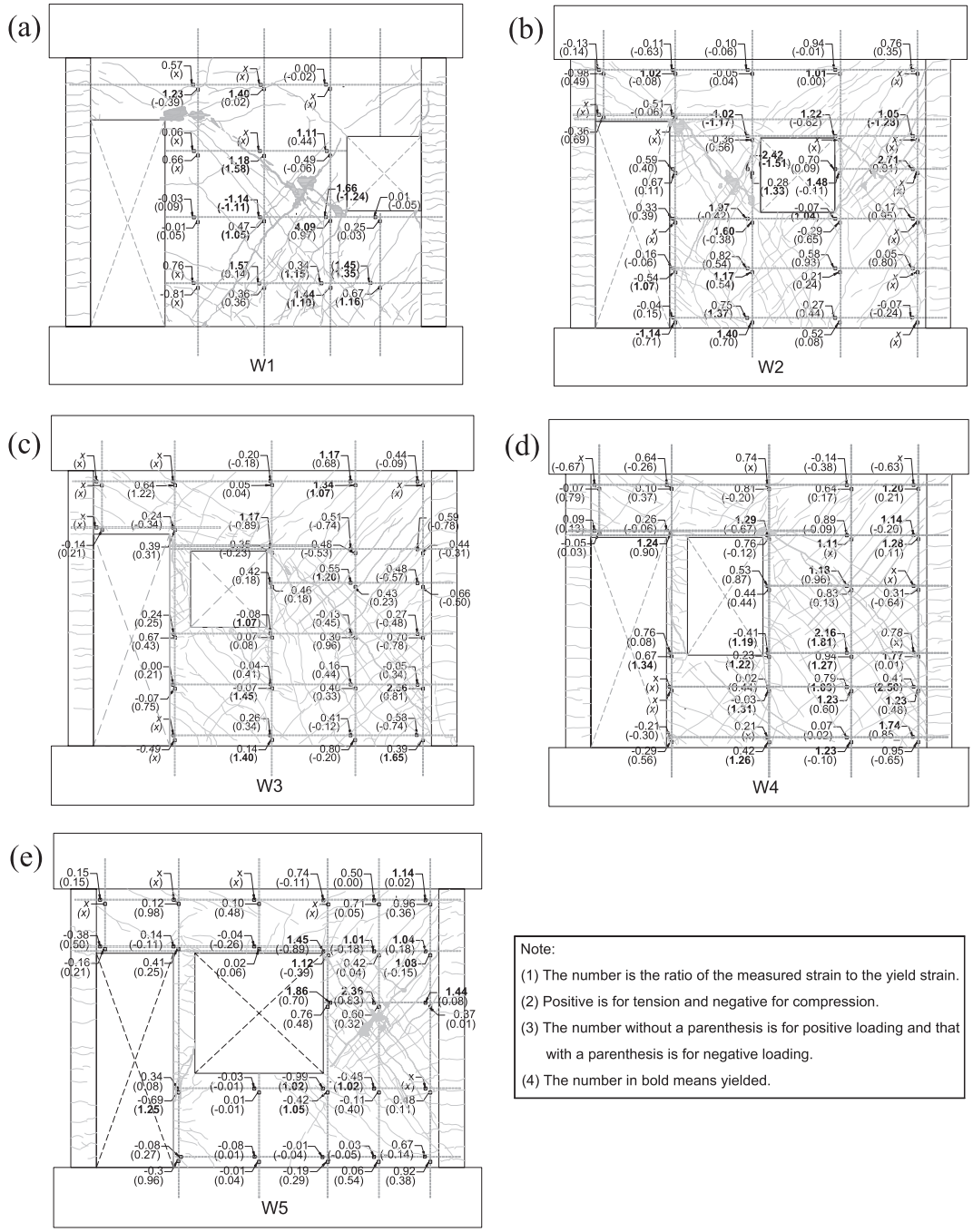

Fig. 8. Ratios of measured strain to yielding strain of web reinforcement at peak lateral force: (a) W1, (b) W2, (c) W3, (d) W4, and (e) W5.

calculating the yield and ultimate strengths, concrete is assumed to take no tension.

3.3. Shear strength

The shear strengths of each element are calculated for cracking and ultimate conditions. The shear cracking strength is the strength at the diagonal cracking, which is the shear strength of concrete V_c based on the ACI code [11]. For walls under axial compression and tension, the V_c is equal to the lesser of Eqs. (1) and (2) (from Table 11.5.4.6 of ACI 318-14 [11]). For columns under compression, the V_c is equal to the lesser of Eqs. (3) and (4) (from Table 22.5.6.1 of ACI 318-14 [11]). For columns under tension, the V_c is calculated by Eq. (5) (Eq. 22.5.7.1 of ACI 318-14 [11]). In this research, the vertical frame element that is formed entirely by a boundary column is considered as a column. The other vertical elements are either formed entirely by the wall web or formed in part by the wall web and in part by the boundary column. They are considered as walls. Other types of equations of V_c are available in the ACI code for walls and columns. Eqs. (1)–(5) are selected because they include the axial force effect.

$$V_c = 0.27\sqrt{f'_c}\, b_w d + \frac{N_u d}{4l_w} \text{ (MPa)} \tag{1}$$

$$V_c = \left(0.05\sqrt{f'_c} + \frac{l_w\left(0.1\sqrt{f'_c} + 0.2\frac{N_u}{l_w b_w}\right)}{M_u/V_u - 0.5l_w}\right) b_w d \text{ (MPa)} \tag{2}$$

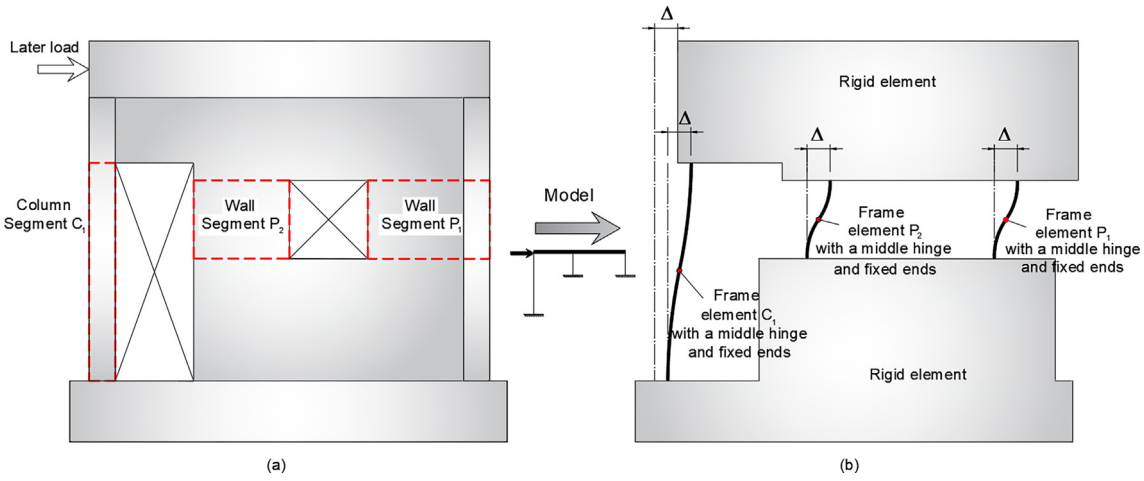

Fig. 9. Proposed structural model: (a) critical segments and (b) analytical model.

$$V_c = 0.29\sqrt{f_c'}\, b_w d \sqrt{1 + \frac{0.29N_u}{A_g}} \text{ (MPa)} \tag{3}$$

$$V_c = \left(0.16\sqrt{f_c'} + 17\rho_w \frac{V_u d}{M_u - N_u \frac{(4h-d)}{8}}\right) b_w d \text{ (MPa)} \tag{4}$$

$$V_c = 0.17\left(1 + \frac{N_u}{3.5A_g}\right)\sqrt{f_c'}\, b_w d \text{ (MPa)} \tag{5}$$

where f_c' = compression strength of concrete; b_w = width or thickness of a vertical element, mm; d = distance from the extreme compression fiber of the section of a vertical element to centroid of tension reinforcement, taken as 0.8 times of the length l_w of a wall element or depth h of a column element; N_u = axial force which is taken as positive for compression and negative for tension; M_u = moment at the critical section; V_u = shear force at the critical section; ρ_w = ratio of the area of tension reinforcement A_s to $b_w d$; h = overall depth of a column element; A_g = gross area of the section.

When using Eqs. (1) and (2) for the critical wall segment that includes the wall web and the boundary column, the b_w is the width of the wall web and l_w is the length of the web plus the overall depth of the column. In Eqs. (3) and (4), the moment M_u and shear V_u are obtained from the critical section away from the ends of the member at a distance, the lesser of $l_w/2$ and $0.5l/2$ for walls [11] or the lesser of d and $0.5l/2$ for columns [12], where l = height of a wall or a column. When the value of $M_u/V_u - 0.5l_w$ in Eq. (2) or $M_u - N_u[(4h - d)/8]$ in Eq. (4) is negative, Eqs. (1) and (3) should be used, respectively. The shear ultimate strength V_n is calculated by V_c plus shear strength contributed by shear reinforcement V_s, which is determined by Eq. (6).

$$V_s = \frac{A_v f_{yt} d}{s} \tag{6}$$

where A_v = area of transverse reinforcement within spacing s; f_{yt} = specified yield strength of transverse reinforcement; s = center-to-center spacing of transverse reinforcement. Based on the ACI code [11], the V_n has a upper limit of $0.83\sqrt{f_c'}$ (MPa) for walls and the V_s has an upper limit of $0.66\sqrt{f_c'}\, b_w d$ (MPa) for columns.

3.4. Shear friction strength

The shear friction strength is calculated by Eq. (7) based on the ACI 318-14 code [11]. The second term in Eq. (7) is to reflect the effect of compression across the shear plane. The shear friction strength should not exceed the least of $0.2f_c'A_c$, $(0.33+ 0.08f_c')A_c$, and $11A_c$ (MPa)

$$V_{fr} = \mu(A_{vf} f_y + N_u) \tag{7}$$

where μ = coefficient of friction; A_{vf} = area of shear-friction reinforcement; f_y = specified yield strength of shear-friction reinforcement.

3.5. Deformation

The deformation of each vertical frame element consists of flexural and shear deformations. The flexural deformations corresponding to the flexural cracking, yielding, and ultimate strengths are calculated from curvatures. Each element is assumed to be bent in double curvatures with a point of zero curvature at the midheight of the element. At the cracking and yielding conditions, the curvature is assumed to have a linear distribution along the element. At the ultimate condition, the concept of plastic hinge length is used to calculate the plastic deformation. The deformation is contributed from a linear curvature distribution along the element with the maximum value equal to the yield curvature and from a maximum plastic curvature uniformly distributed over a plastic hinge length [13]. The value of the plastic hinge length is calculated by Eq. (8) [13].

$$l_p = 0.08\left(\frac{l}{2}\right) + 0.022 d_b f_y \text{ (MPa)} \tag{8}$$

where l_p = plastic hinge length; l = height of a wall or a column; d_b = diameter of longitudinal reinforcement; and f_y = specified yielding strength of longitudinal reinforcement.

The shear deformation before diagonal cracking is calculated by Eqs. (9) and (10) [14]. After diagonal cracking, the shear deformation is calculated by Eqs. (11) and (12), which were first derived from a simplified truss model for beams [14] but were later successfully applied to walls [15]. Note that the angle of diagonal cracks are assumed to be 45 degrees in Eq. (12).

$$\Delta_{suc} = \frac{V}{K_{suc}} \tag{9}$$

$$K_{suc} = \frac{0.4E_c b_w d}{fl} \tag{10}$$

$$\Delta_{sc} = \frac{V - V_c}{K_{sc}} \tag{11}$$

$$K_{sc} = \frac{\rho_h}{1 + 4\frac{E_s}{E_c}\rho_h} \frac{E_s b_w d}{l} \tag{12}$$

where V = applied shear; Δ_{suc} = shear deformation of an uncrack element; K_{suc} = shear stiffness of an uncracked element; E_c = modulus of elasticity of concrete; f = factor to account for the nonuniform distribution of shear stress, for rectangular sections f = 1.2, and for T or I

sections $f = 1.0$; Δ_{sc} = shear deformation of a crack element; K_{sc} = shear stiffness of a cracked element; ρ_h = ratio of area of transverse reinforcement A_s to sb_w; E_s = modulus of elasticity of transverse reinforcement.

3.6. Axial force

In addition to the shear and moment, the axial force in each vertical frame element also has to be determined as it affects the flexural, shear and shear friction capacities of the element. To solve for the axial force acting on each vertical element under a lateral load, the cantilever assumption is adopted. All the vertical elements of the proposed structural model are assumed to form a cantilever column. The axial stress on the cross section of the cantilever column, formed by the cross sections of the vertical elements, is distributed linearly from the tension zone to the compression zone and is assumed to be zero at the neutral axis of the cross section. With this assumption, for a given lateral force on the wall, the axial force in each vertical element can be determined by equilibrium.

3.7. Experimental verification

To calculate the lateral strength of the wall, the force-deformation curve of each vertical frame element of the structural model of the wall is established first with an assumed distribution of axial force in each vertical element. The vertical element that fails first is then identified and the corresponding top displacement determined. With the same top displacement, the shears acting on the other vertical elements are determined from their force-deformation curves. The lateral strength of the wall can be found by summing the shears of all the vertical elements. Meanwhile, the axial force in each vertical element is calculated based on the cantilever column assumption. If the axial force distribution is close to the assumed one, then the analysis is terminated and the strength of the wall is found. Otherwise the calculation is repeated with the obtained axial force distribution as the assumed axial force distribution in the next iteration of calculation.

Fig. 10(a)–(b) and (c)–(d) show the relationship between the top lateral displacement and shear in each vertical frame element for W3 and W4, respectively. For both walls, the lateral strength is governed by the shear strength of element P1, which has the highest lateral stiffness and strength. From the displacement and shear relationships, it can be seen that when element P1 fails in shear, other segments have not reached their ultimate states. At this condition, the shear in element P2 of both W3 and W4 has exceeded the diagonal cracking strength. In contrast, the shear in element C1 is low and does not exceed the diagonal cracking strength but exceeds flexural cracking strength. It exceeds more in the negative direction than the positive direction. This is because tensile stress from flexure is increased by axial tension in the negative direction while decreased by axial compression in the positive direction. These analysis observations are consistent with experimental observations shown in Fig. 5, in which clear diagonal cracks were observed for element P1. In contrast, no significant diagonal cracks were observed for element C1 as shown in Fig. 5. Almost all the cracks were close to horizontal and occurred mostly during negative loading when the element was subjected to axial tension in addition to flexural tension.

The ratios of the experimental lateral strength and the lateral strength calculated by the proposed model of all the specimens are shown in Fig. 11(a) and listed in the second column of Table 3. The ratios are all larger than one with a mean value of 1.62, meaning the proposed calculation is conservative for all the specimens. The ratio for the positive direction of W1 is much lower than those of the others. It is likely because the critical wall segment W1 in the positive direction receives much fewer confinement from the boundary column or other wall segments than the other direction and the critical wall segments of other specimens. The critical wall segment in the compression side is bordered by a large opening, the door, and is bordered by the window in the tension side.

In addition to the proposed model, three simplified models are also examined herein. Simplified model 1 is the same as the proposed model except that the change of axial force is not considered. Therefore, iteration effort for axial force is not needed. Simplified model 2 is the same as model 1 but calculates the lateral strength of the specimen simply by summing the strengths of all the vertical elements. Therefore,

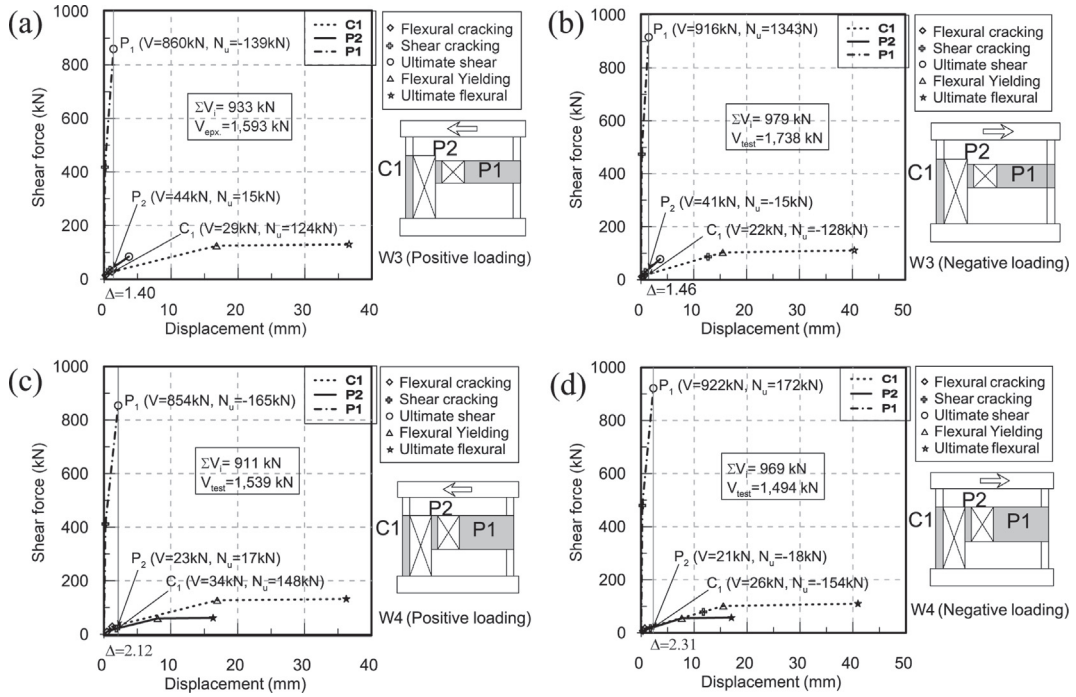

Fig. 10. Calculation of lateral strength: (a) W3 under positive loading, (b) W3 under negative loading, (c) W4 under positive loading, and (d) W4 under negative loading.

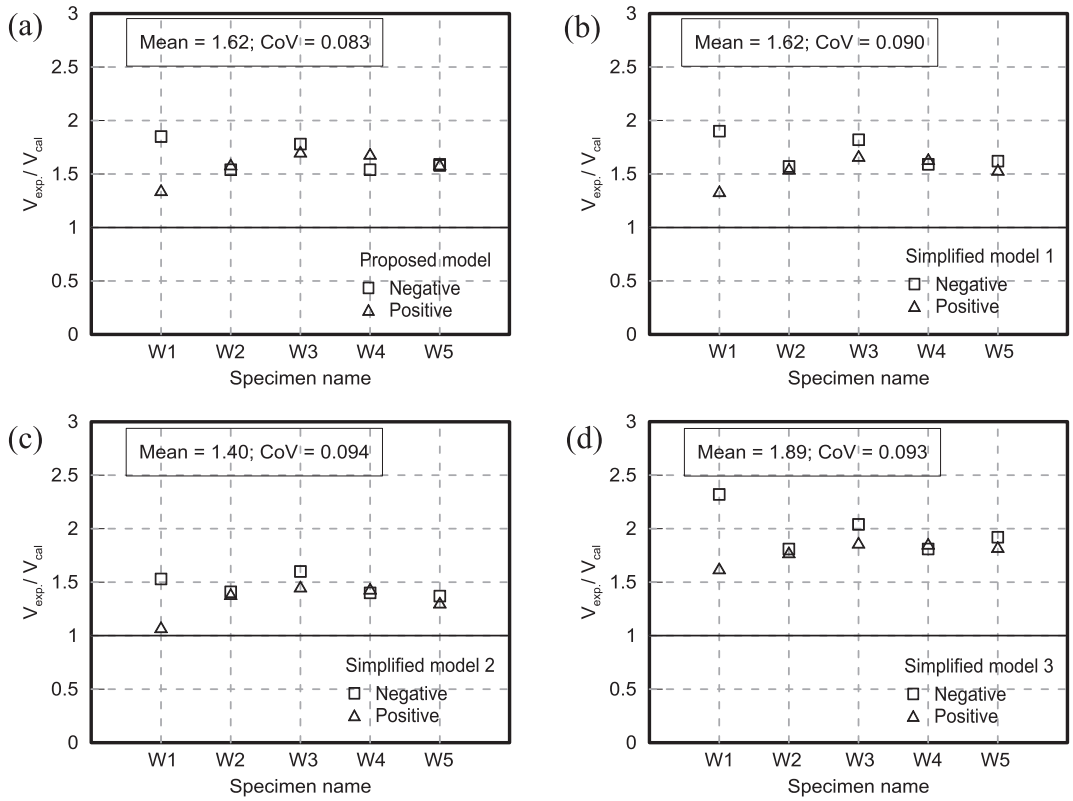

Fig. 11. Experimental to calculated lateral strengths: (a) proposed model, (b) simplified model 1, (c) simplified model 2, and (d) simplified model 3.

the calculation of stiffness and deformation of each element is not required. Only the ultimate strength is calculated for each element. Computational effort can be further reduced. Simplified model 3 is the same as model 2 except that only the wall web is considered in the strength calculation. This is to consider the fact that shears taken by the boundary columns are not as significant as that taken by the wall web. Calculation results for simplified models 1, 2, and 3 are shown in Fig. 11(b), (c) and (d) and listed in the third, fourth and fifth column of Table 3, respectively. It can be seen that the mean value of the ratios of experimental to calculated strengths is 1.62 for simplified model 1, same as that of the proposed model. However, the covariance is increased from 0.083 to 0.090, meaning the scatter of the prediction is increased. For simplified model 2, the mean value of the ratios is reduced to 1.40. This is expected as all the vertical elements in the model are assumed to reach their lateral strengths simultaneously, but in fact the shears taken by columns or slender wall webs when the wall reaches the lateral strength are small as shown in Fig. 10. The covariance is 0.094, greater than the original model and simplified model 1. For simplified model 3, a significant increase of the mean value to 1.89 can be seen. The covariance is 0.093. With the least computational effort, simplified model 3 shows the most conservative and relatively large scatter prediction among all the models examined.

4. Conclusions

Five full-scale reinforced concrete squat walls with openings typical of the first story backside side exterior walls of row houses in Taiwan were tested using lateral cyclic loading to examine their seismic behavior. To estimate the lateral strength of the walls, a detailed model and three simplified models were proposed and verified by the experimental results. Major conclusions are summarized as follows.

(1) It was observed that the wall with the window opening on the side of the wall web (specimens W1 and W3) showed a higher average lateral strength than that with the opening placed around the center of the wall web (specimen W2). This is likely because the critical wall segment of the former had a lower height to length ratio than the latter and hence can transfer lateral load more efficiently with a diagonal strut that is less steep. The increase of the opening length reduced more the lateral strength than the increase of the opening height. This is because the former not only increased the height to length ratio of the critical wall segment (same as the later) but also

Table 3
Experimental to calculated lateral strengths.

Specimen	Proposed		Simplified 1		Simplified 2		Simplified 3	
	Positive	Negative	Positive	Negative	Positive	Negative	Positive	Negative
W1	1.35	1.85	1.34	1.90	1.08	1.53	1.63	2.32
W2	1.59	1.54	1.55	1.57	1.39	1.41	1.78	1.81
W3	1.71	1.87	1.67	1.82	1.46	1.60	1.87	2.04
W4	1.69	1.54	1.64	1.59	1.44	1.40	1.86	1.81
W5	1.59	1.58	1.54	1.62	1.31	1.37	1.83	1.92
Mean	1.62		1.62		1.40		1.89	
CoV	0.083		0.090		0.094		0.093	

reduced the cross-sectional area of the critical wall segment. A critical wall segment tended to show a lower lateral strength when the edge of the segment is bordered by a door than by a boundary column due to the confinement effect provided by the column.

(2) A lateral strength model is proposed for the wall specimens tested. Comparison with the test results shows that the proposed model can be conservatively used to predict the lateral strength of the wall specimens. Three simplified models with less computational effort are also proposed. Comparison with the test results shows that ignoring the variation of the axial force among the wall segments and columns of the model does not change the average prediction but increases the scatter of prediction (simplified model 1). Simply summing the lateral strengths of all the wall segments and columns together and without considering the variation of axial force further increases the scatter and greatly reduces the degree of conservatism (simplified model 2) as compared with original model. Summing the lateral strengths of all the web segments only and without considering the variation of axial force requires the least computational effort but greatly increases the degree of conservatism and the scatter of prediction as compared with the original model.

Acknowledgements

The authors would like to thank the financial support from the Architecture and Building Research Institute (ABRI) and the Ministry of Science and Technology (MOST) of Taiwan under Contract Nos. 106-2221-E-002 -233 -MY3. In addition, this research was partially supported by the Basic Science Research Program through the National Research Foundation of Korea (NRF) funded by the Ministry of Education, Korea (Grant No. 2018R1D1A1B07048759).

References

[1] Kabeyasawa T, Kimura T. Ultimate strength reduction of reinforced concrete shear walls with an opening. Concr Eng Ann Meet 1989;11:585–90. [in Japanese].
[2] Li Bing, Pan Z, Zhao Y. Seismic behaviour of lightly reinforced concrete structural walls with openings. Mag Concr Res 2015;67:843–54.
[3] Ono M, Tokuhiro I. A proposal of reducing rate for strength due to opening effect of reinforced concrete framed shear walls. J Struct Constr Eng 1992:119–29. [in Japanese].
[4] Lin CY, Kuo CL. Behavior of shear wall with openings. Proceedings of ninth world conference on earthquake engineering, Tokyo-Kyoto, Japan, 4. 1988. p. 535–40.
[5] Bing Li K, Qian HWu. Flange effects on seismic performance of reinforced concrete squat walls with irregular or regular openings. Eng Struct 2016;110:127–44.
[6] Massone Leonardo M, Munoz Gonzalo, Rojas Fabian. Experimental and numerical cyclic response of RC walls with openings. Eng Struct 2019;178:318–30.
[7] Taylor Christopher P, Cote Paul A, Wallace John W. Design of slender reinforced concrete walls with openings. ACI Struct J 1998;95(4):420–33.
[8] Ono M, Tokuhiro I. Study on estimate of the shear strength of reinforced concrete framed shear walls with opening. Concr Res Technol 1996;7:53–64. [in Japanese].
[9] Architectural institute of Japan. AIJ standard for structural calculation of reinforced concrete structures. Tokyo (Japan): Architectural institute of Japan; 2010. [in Japanese].
[10] Sakurai M, Kuramoto J, Matsui T. Shear strength evaluation for RC shear walls with multi-openings based on FEM analysis. 15 world conference on Earthquake engineering (15 WCEE), Lisbon. 2012. p. 4635–44.
[11] American Concrete Institute. ACI 318-14 building code requirements for structural concrete and commentary (Metric). American Concrete Institute; 2014.
[12] ACI-ASCE Committee 326. Shear and diagonal tension. J Proc 1962.
[13] Paulay Thomas, Priestley Micheal JN. Seismic design of reinforced concrete and masonry buildings. John wiley & sons, INC; 1992.
[14] Park Robert, Paulay Thomas. Reinforced concrete structures. John Wiley & Sons, Inc.; 1975.
[15] Li Bing, Xiang Weizheng. Effective stiffness of squat structural walls. J Struct Eng 2011;137:1470–9.